A comparative study on the performance of radiation detectors from the HgI$_2$ crystals grown by different techniques

João F. T. Martins,
Fabio E. Costa,
Robinson A. dos Santos,
Carlos H. de Mesquita,
Margarida M. Hamada

Abstract. In this work, the establishment of a technology for HgI$_2$ purification and crystal growth is described, aiming at a future application of this crystal as a room temperature radiation semiconductor detector. Two methods of crystal growth were studied in the development of this work: (1) physical vapor transport (PVT) and (2) saturated solution from dimethylsulphoxide (DMSO) complexes. In order to evaluate the crystals obtained using each of these methods, systematic measurements were carried out for determining the stoichiometry, structure, orientation, surface morphology and impurity of the crystal. The influence of these physicochemical properties of the crystals developed was evaluated in terms of their performance as a radiation detector. The best response to radiation was found for the crystals grown by the PVT technique. Significant improvement in the performance of HgI$_2$ radiation detector was found, purifying the crystal by means of two successive growths by the PVT technique.

Key words: crystal growth • iodide mercury crystal • physical vapor transport (PVT) • radiation detector • semiconductor crystal

J. F. T. Martins, F. E. Costa, R. A. dos Santos,
C. H. de Mesquita, M. M. Hamada✉
Institute for Nuclear and Energy Research
(IPEN-CNEN/SP),
2242 Prof. Lineu Prestes Ave., Cidade Universitária,
05508-000, São Paulo – SP, Brazil,
Tel.: +55 11 3133 9779, Fax: +55 11 3133 9765,
E-mail: mmhamada@ipen.br

Introduction

There have been attempts to develop room temperature X- and gamma-ray semiconductor detectors for various applications. Over the past decade, new compound semiconductors, with properties suitable to be used as room temperature detectors, have been studied to be developed as possible alternatives to Si and Ge semiconductors for charge particle and photon detection [13, 16, 18]. The application of these detectors has been somewhat restricted, since Ge detectors provide high-resolution capabilities only at cryogenic temperatures (77 K), because of their low resistivity at room temperature, and Si detectors exhibit sufficient detection efficiency only for low energy rays (less than 20 keV), due to their low photon stopping power at higher energies. Thus, there has been a strong interest in developing semiconductors that have high photon stopping power and may operate at room temperature. The main physical semiconductor properties required for fabrication of room temperature semiconductor detectors are: (1) high atomic number; (2) high density; (3) high absorption coefficient; (4) a band gap large enough to keep leakage currents low, at room temperature and (5) large electron and hole mobility-lifetime products, for an efficient charge collection [7, 13, 16, 18]. Among these types of detectors, HgI$_2$ has emerged as a particular interesting material in view of its wide band gap (2.13 eV) and its large density (7.5 g/cm^3). HgI$_2$ crystals

are composed of high atomic number elements (Z_{Hg} = 80 and Z_I = 53) and have high resistivity (>10^{14} Ω·cm) [13]. These are important factors in applications where compact and small thickness detectors are necessary for X- and gamma-ray measurements. However, the applications of HgI_2 are limited by the difficulty in obtaining high-quality single crystals [7, 13, 16, 18].

There is agreement in the literature on the difficulty in growing crystals with high crystallographic perfection, high chemical purity and good stoichiometry, suitable to be used as room temperature semiconductor detectors [4, 8, 9, 13, 16, 18]. These basic requirements should be met at various stages in the manufacture of the detector. The procedures for obtaining the radiation semiconductor detector comprise: (a) purification of the starting material, (b) crystal growth, (c) crystal surface preparation, (d) preparation of ohmic contacts, (e) mounting on a rigid substrate and (f) detector encapsulation. Each of these stages can affect the crystalline quality and introduce defects and imperfections, deteriorating the radiation detector response [4, 7–9, 13, 16, 18].

Several studies [1–4, 6, 10, 11, 14, 20–24, 26] have been carried out about the preparation of the HgI_2 semiconductor detector and progresses have been made by the improvement of the techniques of purification, growth and characterization of the crystal. However, problems still exist and to grow HgI_2 crystals with suitable purity to be used as a room temperature radiation detector is a technological challenge. The impurities, which act as charge carriers trap, influence the charge carrier lifetime, affecting the detector efficiency [1, 6, 11, 26].

Most semiconductor crystals are grown by the fusion technique. However, the HgI_2 undergoes structural phase transition below its melting point (259°C), what makes its growth by fusion technique [10, 14] more difficult compared to PbI_2 (405°C) and $TlBr$ (468°C). Thus, other techniques, such as physical vapor transport (PVT) [2, 24, 26] or saturated solution [20, 23] are more recommended for the growth of HgI_2.

In this work, two methods were developed for the HgI_2 growth, namely, the physical vapor transport (PVT) [22, 23] and the saturated solution from dimethylsulphoxide (DMSO) complex methods. The obtained crystals by the two methods were characterized considering the following physical chemistry properties: crystal stoichiometry, crystal structure, orientation of crystallographic plane, crystal surface morphology and crystal impurity. The influence of these physical chemistry properties on the crystals developed by the two techniques was studied, evaluating their performance as a radiation detector.

Experimental procedure

The commercially available HgI_2 powders (Alpha Aesar), with a nominal purity of 99.9%, was used as the starting material for growing crystals. The crystals were grown by PVT and DMSO complexes Saturated Solution techniques.

The schematic diagram of the oil-bath furnace, used for HgI_2 crystal growth from PVT is shown in Fig. 1A. For growth, the borosilicate glass ampoules were filled with 5 g of HgI_2 salt, evacuated at 90°C for 15 min and subsequently sealed, aiming the salt dehumidification, the HgI_2 vapor loss prevention and the addition of contaminants. Next, the ampoule containing HgI_2 salt at the bottom is placed in a bath of silicone oil and wrapped in a metal casing. The heated HgI_2 salt sublimes to the upper region of the ampoule, being deposited in the heat exchange region, where the crystalline structure is formed. The raw material residual remained at the ampoule bottom. Following the same procedure, the crystal obtained at the upper region was grown twice, aiming to obtain a purer crystal.

For the DMSO complexes saturated solution technique, 25 g of the HgI_2 salt was added to 250 ml of DMSO solution under constant agitation and a colorless solution was formed. After that, this solution was left to stand covered with a filter paper. Evaporation of the solvent should be quite slow, what is of fundamental importance for the formation of good crystal lattices. As the solvent evaporates, the HgI_2 salt is assembled
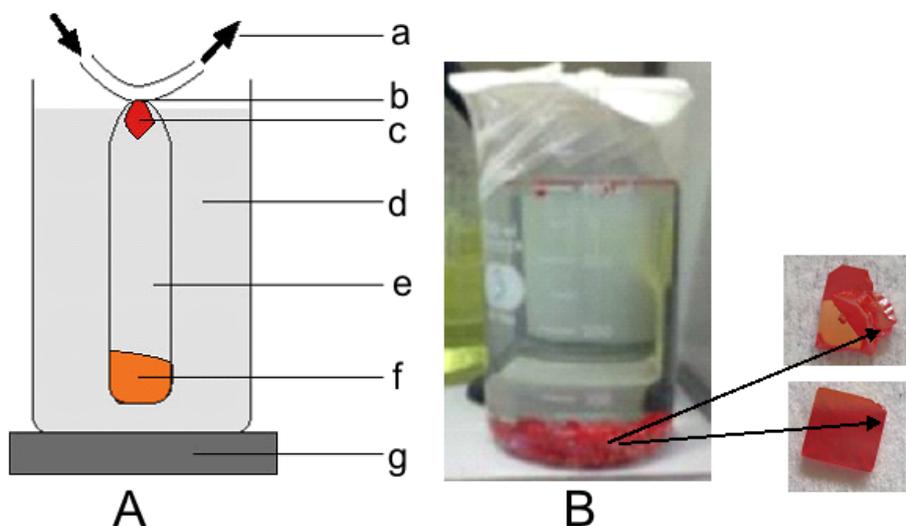
Fig. 1. Schematic diagram of the oil-bath furnace for crystal growth by: (A) PVT technique: (a) water flow for cooling, (b) heat exchange region, (c) crystal, (d) silicone oil, (e) glass ampoule, (f) salt and (g) controllable heating plate and (B) DMSO solution containing HgI_2 crystals and some sampling of the selected crystals from the DMSO saturated solution.

at the bottom of the glass due to its lower solubility and, consequently, the HgI$_2$ solubilized forms crystals (Fig. 1B). The crystals grown in the DMSO solution were selected in terms of their appearance and dimension, as shown in Fig. 1B. The selected crystals were re-grown in order to obtain purer crystals, since impurities are expected at each growth.

For physical-chemistry characterization, the impurity concentration, the surface morphology and the stoichiometry of the HgI$_2$ crystal were analyzed by the scanning electron microscopy with back-scattered electron (SEM-BSE) technique, using the scanning electron microscopy (SEM-BSE), LX 30 Philips model. The crystalline quality and structural characterization of the HgI$_2$ crystal were analyzed by X-ray diffraction (XRD). X-ray diffraction patterns were obtained in a Siemens (D5005) diffactrometer, using CuK$_\alpha$ radiation (2θ ranging from 10 to 100°).

The schematic diagram of the detector and its connection to a preamplifier for radiation response measurements is shown in Fig. 2. For crystal resistance R (MΩ) measurements, the preamplifier (A250F Amptek) input (Fig. 2) was disconnected and the bias current measured with a Keithley Multimeter (mod. 619). Previously, the HgI$_2$ crystals were cleaved and prepared as radiation detectors by the ring electrode paintings. The electrodes were made with colloidal carbon painting, Viatronix™. The electrode areas were 2.5, 24.8 and 10.0 mm^2 for crystals grown by twice PVT, DMSO and once PVT, respectively. The electrode areas were determined from a picture of the crystals contained a well-known reference object. The picture of electrode area was processed in a CAD software (ZWCAD™ 2009i Professional version) being inscribed in a polyline capable of defining its area with an error of 1%. The detector thickness was measured with a micrometer with an uncertainty of ∼20%. The resistivity was calculated using Eq. (1) [12]

$$(1) \qquad \rho = \frac{R \cdot A}{l}$$

where R is the resistance determined by the slope of the curve current (A) vs. bias (V) (Fig. 6), A is the electrode area and l is the thickness of the crystal. The uncertainty Δ_ρ in the resistivity ρ was estimated by Eq. (2):

$$(2) \qquad \Delta_\rho^2 = \left(\frac{\partial \rho}{\partial R}\right)^2 \cdot \Delta_R^2 \left(\frac{\partial \rho}{\partial A}\right)^2 \cdot \Delta_A^2 + \left(\frac{\partial \rho}{\partial l}\right)^2 \cdot \Delta_l^2$$

where Δ_R is the estimated uncertainty for the R parameter, Δ_A is the estimated uncertainty for the area
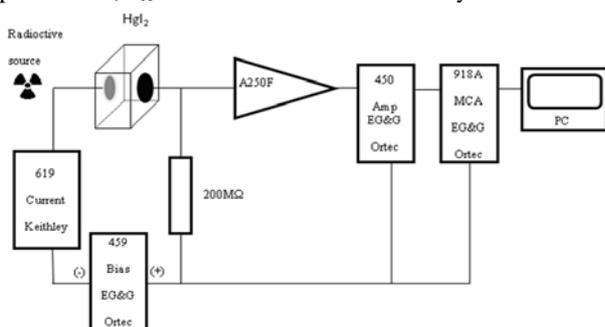
Fig. 2. Diagram of the associated electronics to the HgI$_2$ semiconductor detector for radiation measurements.

determination (assumed as 1%) and Δ_l is the estimation uncertainty for the crystal thickness (assumed as 20%).

For measurements of pulse height spectra, the output from A250F charge sensitive preamplifier was connected to a 450 EG&G Ortec Research Amplifier at 10 μs shaping time and to EG&G 918A multichannel analyzer, to obtain the pulse height spectra. HgI$_2$ crystal detectors were excited under a 59 keV ^{241}Am (400 kBq) gamma source, biased with 150 V (Fig. 2). All measurements were carried out at room temperature, 24 ± 2°C.

The lower limit of detection (LD) is defined as the smallest amount of activity that can be detected with statistical significance. LD can be calculated as [17]

$$(3) \qquad LD \, (cpm) = \frac{3 + 4.65 \times \sqrt{R_B}}{T}$$

where R_B is the background count rate and T is the count time and cpm means counts per minute.

The minimum detectable activity (MDA) is defined as the smallest amount of activity that can be quantified, and it is defined as:
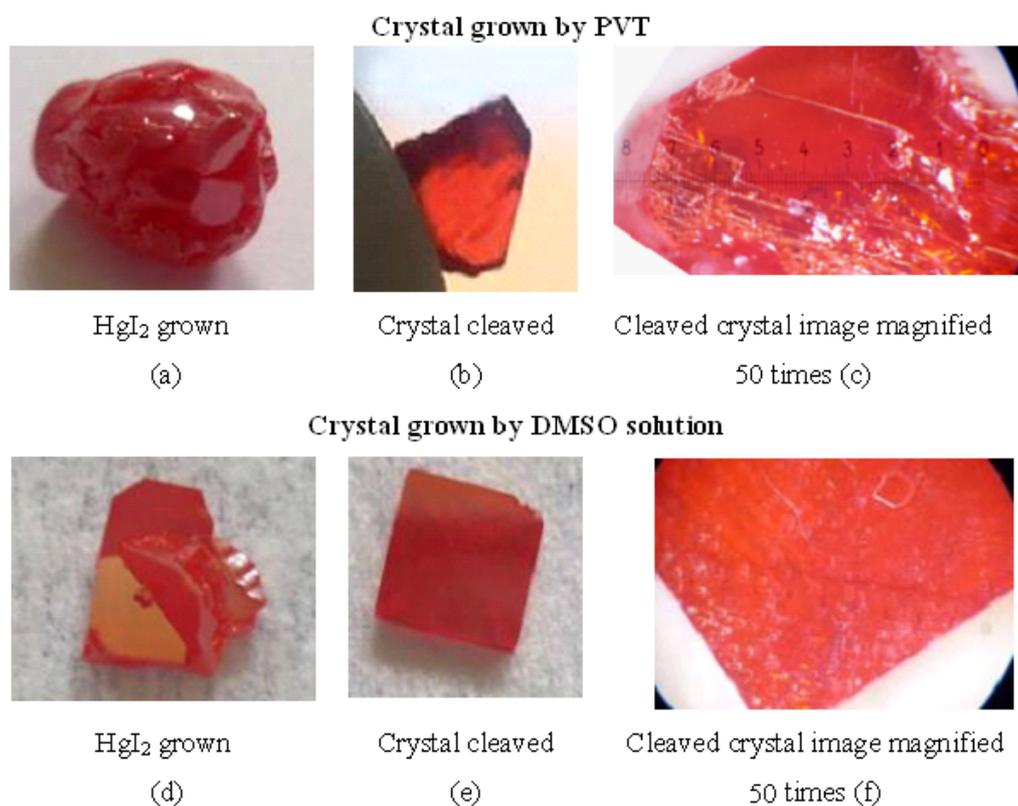
$$(4) \qquad MDA \, (Bq / mm^2) = \frac{LD}{\varepsilon \cdot A \cdot 60}$$

where: ε – counting efficiency; A – electrode area.

Results and discussion

In Fig. 3, the crystal obtained from two successive growths by the PVT method, is shown as it follows: the brilliant dark red colour crystal is grown with a 15 mm maximum diameter and 20 mm in thickness (Fig. 3a), after cleavage (Fig. 3b) and enlarged 50 times with an optical microscope (Fig. 3c): a deep red colour and glossy surface may be observed. The HgI$_2$ crystals obtained by the PVT technique were re-grown twice in order to be purified, since the reduction of impurities is expected at each growth. Figures 3c, 3d and 3e present the crystal re-grown by DMSO solution, cleavage and enlarged 50 times, respectively. Crystals of 1 cm^2 superficial area and 0.5 cm in thickness with regular angulations plus uniform and transparent surface were obtained, as it may be observed in the figure.

The typical X-ray diffraction patterns of the cleavage surface from HgI$_2$ crystals grown by PVT and DMSO techniques are shown in Fig. 4. No significant difference was observed in the diffraction pattern between the crystals grown by both techniques. The results show that the crystals have a similar structure to the tetragonal crystalline pattern of the HgI$_2$. The X-ray diffraction pattern indicates that both crystals are, preferentially, oriented in the (001) and (101) directions. Similar results were found by Ariesanti *et al.* [1]. The lower intensities observed on the diffraction pattern from DMSO crystal (Fig. 4b) could be attributed to the misorientations, absorption related with defects or impurities in the crystal. However, these imperfections seem have not affected the crystal structure, as presented in Fig. 4. Thus, this lower intensity found in DMSO crystals may possibly be due to the superficial defects in the crystal surface. Further studies should be made to understand this behaviour.

Crystal grown by PVT

HgI₂ grown

(a)

Crystal cleaved

(b)

Cleaved crystal image magnified

50 times (c)

Crystal grown by DMSO solution

HgI₂ grown

(d)

Crystal cleaved

(e)

Cleaved crystal image magnified

50 times (f)

Fig. 3. Crystal original form re-grown by PVT (a) after the cleavage (b) and magnified 50× with optical microscope (c). HgI₂ crystal original form re-grown by DMSO complex (d) after the cleavage (e) and magnified 50× with optical microscope (f).
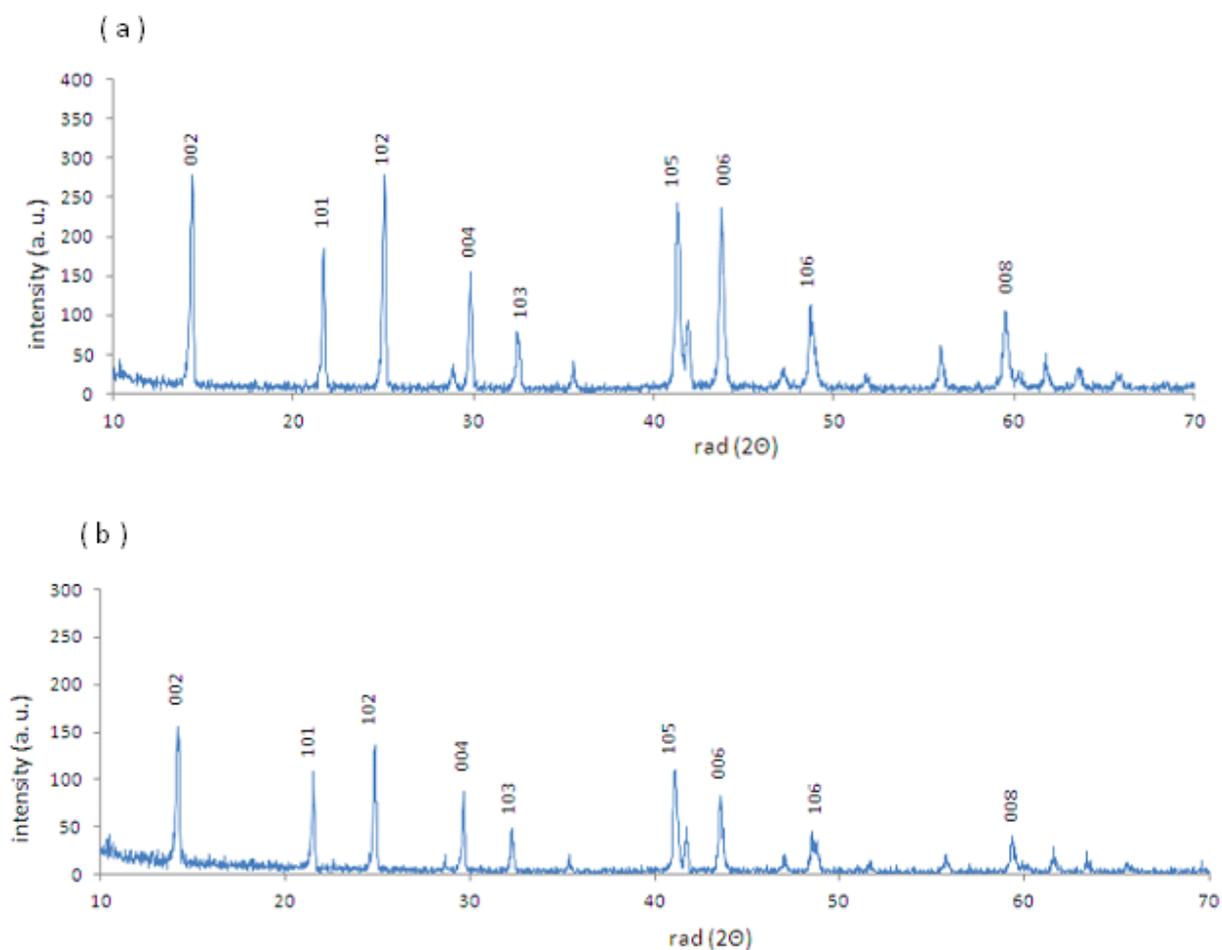
Fig. 4. X-ray diffraction pattern of HgI₂ grown by PVT (a) and DMSO (b) techniques.
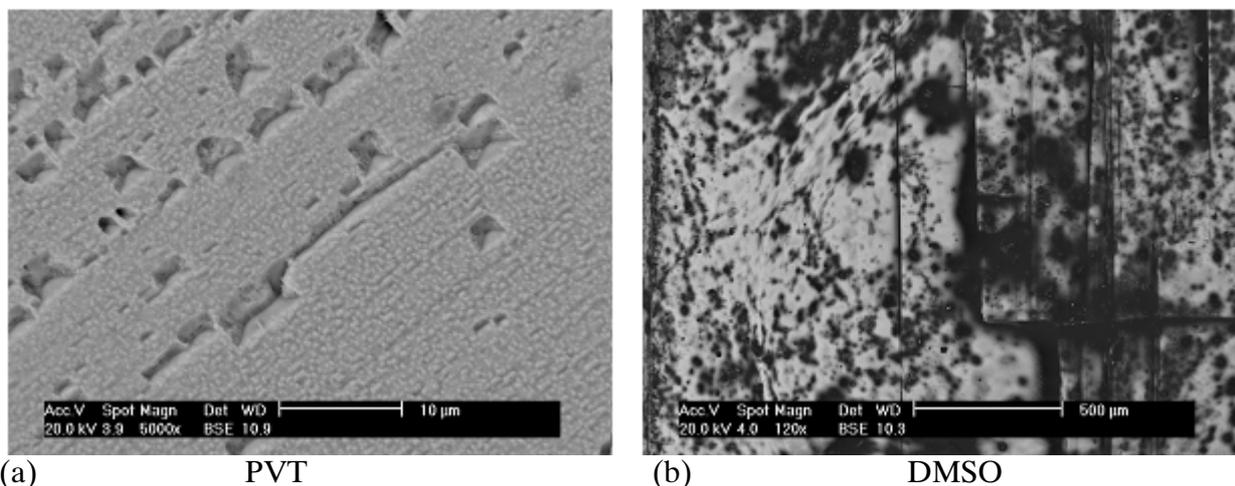
Fig. 5. Micrographs of the HgI$_2$ crystal surface grown by PVT (magnified 5000 times) (a) and DMSO complexes (magnified 120 times) (b).
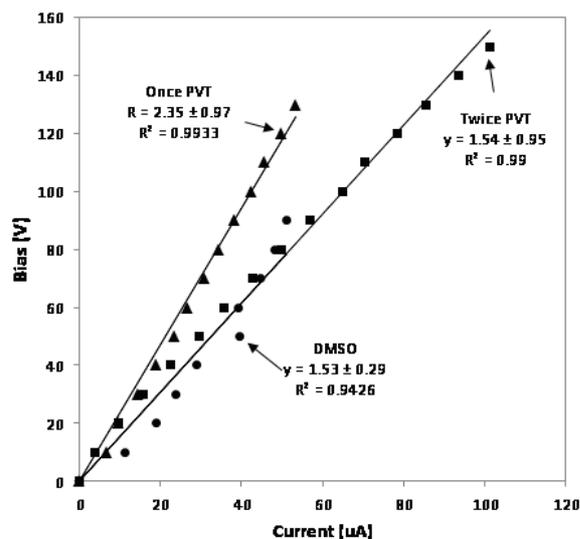
Figure 5 shows the micrographs of the scanning electron microscopy with back-scattered electrons (SEM-BSE) carried out in the HgI$_2$ cleavage wafer from the crystals grown twice by PVT and DMSO complexes, in order to evaluate the quality of the HgI$_2$ cleavage wafer surface. For crystal grown by DMSO, the roughness and the incrustations of the distinct elements may already be detected, clearly, magnifying the image only 120 times (Fig. 5b). On the other hand, for a crystal grown by PVT, a structure with uniform layers may be observed, even magnifying the image 5000 times (Fig. 5a), indicating a good orientation in structure of this crystal.

Additionally, SEM-BSE technique provides a semi-quantitative scanning of the elements present on the surface of the crystal, as well as the stoichiometry of HgI$_2$. The elemental compositions of the crystal surfaces in the HgI$_2$ grown are shown in Table 1. As it can be seen from this table, an appropriate stoichiometry was found. For example, the Hg atomic percentage of the HgI$_2$ crystal grown by PVT was 29.51, while for the I$_2$ it was 55.68 (Table 1a), corroborating a good stoichiometry. Other elements were observed in the trace form, acting as impurities in the crystal. In Table 1 the elemental composition of the HgI$_2$ crystal grown by DMSO complexes is also summarized. Although the suitable stoichiometry of HgI$_2$ (at.% Hg = 28.46, I$_2$ = 54.45) was found, a significant amount of Si was identified (Table 1b). The contents of 21.52% Si in the crystal was not expected, taking into account the trace amount of Si found in the HgI$_2$ salt used for growth

Table 1. Elemental composition of the HgI$_2$ crystal surface grown by PVT (a), DMSO solution (b) and the HgI$_2$ residual salt after the crystal growth by PVT (c)

	Element	Weight (%)	Atomic %	Uncertainty (%)
	(a)			
	O	1.50	12.47	11.90
	Al	0.10	0.49	141.02
Crystal grown by PVT	Si	0.26	1.22	48.97
	Hg	44.65	29.51	1.63
	K	0.18	0.62	58.85
	I	53.30	55.68	1.59
	(b)			
	Si	21.52	59.76	1.43
Crystal grown by DMSO	Hg	35.43	13.78	2.09
	I	43.06	26.46	1.88
	(c)			
	O	23.92	53.28	16.61
	Na	2.11	3.27	1.44
	Mg	1.94	2.84	1.52
HgI$_2$ residual salt from PVT	Al	5.18	6.84	3.84
	Si	2.73	3.47	2.02
	Hg	24.46	4.35	6.54
	K	23.49	21.41	19.99
	I	16.17	4.54	3.65

Fig. 6. Current vs. bias of HgI$_2$ detectors for crystals grown once and twice by PVT and DMSO solution.

as well as that Si values estimated for crystal grown by PVT and its material residual (Table 1). This suggests a Si contamination in the HgI$_2$ crystal from the silicone oil used as heating bath for crystal growth, since in the DMSO technique, the HgI$_2$ salt is immersed in DMSO complex inside an open glass recipient (Fig. 1). Silicone oil is a polymerized siloxane with organic side chains which are formed from alternating silicon-oxygen atoms (...Si-O-Si-O-Si...). Thus, although silicone oil demonstrates temperature-stability and good heat-transfer characteristics, it can have volatilized and contaminated surface of the HgI$_2$ crystal during the growth [15]. From the results of diffraction pattern, as shown in Fig. 4, it can be realized that no modification in structure and orientation of the crystal was presented, suggesting the contamination occur only in the crystal surface. However, a further study should be carried out to understand these results. Furthermore, due to the high intensity of the Si peak in the DMSO crystal, it was not possible to identify the peaks of the other trace elements present as impurities in the PVT crystal.

The elemental composition determination from the residual salt after the crystal growth by PVT was performed to evaluate the efficiency of HgI$_2$ purification by the PVT technique. Samples from the residual HgI$_2$ salt were evaluated by the SEM-BSE technique (Table 1c) and compared with those obtained for the HgI$_2$ crystal grown twice by PVT (Table 1a). The presence of significant amounts of impurities can be observed, namely, O, Na, Mg, Al, Si, K, mainly potassium (21.41%) and oxygen (53.28%), which were higher than those of Hg (4.35%) and I (4.54%). The stoichiometry of HgI$_2$ was not followed in this sample, contrary to that found in the HgI$_2$ crystal grown. This result demonstrates the efficacy of the PVT technique to purify the starting material.

After the HgI$_2$ crystal preparation as a radiation detector, its performance in response to radiation was carried out. The function between the applied bias vs. leakage current for the crystal grown by PVT and DMSO solution techniques are shown in Fig. 6. The resistivity determined for the grown crystals are summarized in Table 2. As it can be observed in Fig. 6 and Table 2, the leakage current of the crystal grown twice by the PVT technique allowed to apply a higher voltage to the detector, despite the resistivity value of the HgI$_2$ crystal grown twice by PVT technique, which is lower (85 MΩ·cm) when compared to the values of the crystals grown by PVT once (440 MΩ·cm) and the DMSO solution (640 MΩ·cm). These resistivity values are close to that obtained experimentally by other authors [5, 23]. Applying a higher voltage on the twice PVT crystal, the charge carriers produced by radiation may be collected more easily, resulting in detectors with better efficiency. Also, it should be emphasized that the crystals grown twice by PVT present a high correlation between the current and bias values up to 140 V bias, while crystals grown once by PVT and DMSO solution presented high noise above 130 V and 90 V, respectively. It is important to emphasize that crystals operating at higher voltages accelerate the charge carriers and facilitate their collection.

The response of radiation detectors produced by PVT and DMSO procedures is shown in Table 2. The detector crystal prepared from the purified HgI$_2$ salt, subjected to two growths by PVT was sensitive to alpha and gamma radiation and very sensitive to light, while those from the crystal grown once by PVT (not purified) showed less sensitivity to light, probably due to the presence of impurities in higher concentrations. The detector prepared with the crystal grown by the DMSO saturated solution was only sensitive to alpha radiation and light. The low sensitivity of the detector from the HgI$_2$ crystal obtained by DMSO may be due to a higher amount of impurities in the crystal, combined with roughness and a non-uniform surface, as shown in Fig. 5.

Figure 7 illustrates the pulse height spectrum obtained for HgI$_2$ grown twice by PVT, using a ^{241}Am gamma source (59 keV) for the crystal excitation. Previously, the measurement was carried out to evaluate the background radiation (BKG) and the electronic noise, as shown in the bottom curve in Fig. 7. Thereafter, the spectrum of a ^{241}Am (400 kBq) was performed to establish the quality of the crystal to operate as a low--energy detector. The detection limit, LD, was equal to 6.72 counts per minute (cpm) and the minimum detectable activity (MDA) was 2.05 Bq/mm^2. As it can be observed from this figure, the twice PVT detector was capable of presenting radiation response and pulse height with recognizable features under gamma-ray excitation. Although the resolution FWHM (full width at half maximum) at the 59 keV peak, considering only the right side was, ~11%, which can be considered relatively poor compared with that described in the literature for other

Table 2. Radiation response of the HgI$_2$ detectors grown by different procedures

	HgI$_2$	HgI$_2$	HgI$_2$
Crystal growth method	Purified PVT (grown twice)	PVT (grown once)	DMSO
Sensibility	α, γ and light	α, γ and light	α and light
Resistivity	8.5×10^7 Ω·cm	4.4×10^8 Ω·cm	5.9×10^8 Ω·cm
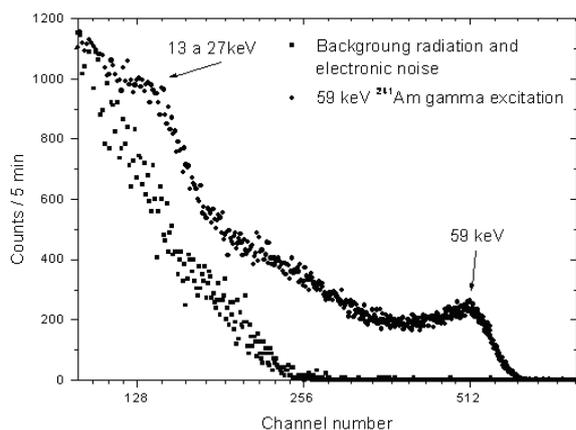
Fig. 7. Channel spectrum of the HgI$_2$ crystal grown twice by PVT, under ^{241}Am gamma-rays excitation.

promising room temperature semiconductor detectors, like TlBr (FWHM ~4%) [19] and CdTe (FWHM ~2%) [25]. To obtain better resolution, it is necessary to improve the charge collection [1]. This goal may be achieved by improving: (a) salt purification in order to decrease the charge traps, (b) detector electrodes, (c) surface treatment. A continuous effort for overcoming these suggestions can be observed in the literature and improvements have been achieved in the fabrication technology of HgI$_2$ detector [1, 2, 6, 14, 23, 24]. However, there are still limitations that inhibit their commercial availability and remain a technological challenge and study purpose of the major international centers. For the HgI$_2$ crystal grown by DMSO saturated solution, no radiation response was observed when excited with gamma radiation, probably due to the interference of the high leakage current in the occasional radiation signal detection. It was possible to observe the radiation response only under ^{241}Am alpha radiation (5.4 MeV) in the current mode. The detection, in the pulse mode, was not observed due to the low radiation response and high noise signal. Further studies should be performed to evaluate the influence of the crystal impurities and crystalline quality on the detector performance.

A better performance was found for the crystal grown twice by the PVT technique compared with that grown once (without purification), although its resistivity was smaller, what may be attributed to its better purity, which allows to apply higher voltage. Thus, the charge carriers produced by radiation can be collected more easily, achieving better detector efficiency.

For more accurate information on the performance of HgI$_2$ radiation detectors, concerning trace impurities present in the crystal, more studies evaluating the response of the detector, in each purification process, are necessary. It is expected that detectors with better resolution may be obtained using crystals with high purity, what, consequently, increases the collection charge.

Conclusion

The HgI$_2$ crystals grown by PVT method presented better performance as radiation detectors compared to the DMSO solution. Also, the PVT was effective to reduce the concentration of HgI$_2$ impurities. The HgI$_2$ crystal grown by PVT presented pulse height with recognizable features under gamma-ray excitation, although the resolution was poor. The detection limit, LD, was equal to 6.72 cpm and the MDA was 2.05 Bq/mm^2. On the other hand, for the HgI$_2$ crystals, grown by DMSO solution, no radiation response was observed under gamma-ray excitation.

The response to radiation presented by HgI$_2$ crystals grown still need to be improved. The resolution FWHM of 11% at the 59 keV peak can be considered relatively poor compared with that described in the literature for other promising room temperature semiconductor detectors, like TlBr and CdTe. The efficiency and the energy resolution of the detectors have been currently limited by incomplete charge collection. Further improvement of the detector performance can be achieved by investigating structural and surface properties, by optimizing the purification and growth techniques and progress in measurement conditions.

References

1. Ariesanti E, Kargar A, McGregor DS (2010) Fabrication and spectroscopy results of mercuric iodide Frisch collar detectors. Nucl Instrum Methods Phys Res A 624;3:656–661
2. Ariesanti E, Kargar A, McGregor DS (2010) Vapor growth of tetragonal prismatic mercuric iodide crystals. In: Nuclear Science Symposium Conference Record (NSS/MIC), 2010 IEEE, Knoxville, USA, 1:3739–3745
3. Ayres F, Machado WVM, Justo JF, Assali LVC (2003) Defects in mercuric iodide: an APW investigation. Physica B 340:918–922
4. Coleman CC (1970) Growth of large HgI$_2$ single crystals. J Cryst Growth 6;2:203–204
5. Cummings T, Marin C, Ostrogorskya AG, Burgerc A, Blissd M (2006) Tetragonal red and yellow HgI$_2$-CdI$_2$ crystals for X- and γ-ray solid-state detectors directionally solidified under argon pressure of 20 atm. J Cryst Growth 297:334–338
6. Gang X, Wanqi J, Gaohong L, Xiaoyan S (2010) Heat treating and detectors characterization of α-HgI$_2$. Rare Met Mater Eng 39;12:2088–2090
7. Heller S, Zanzonic P (2011) Nuclear probes and intraoperative gamma cameras review article. Semin Nucl Med 41;3:166–181
8. Hitomi K, Muroi O, Shoji T, Suehiro T, Hiratate Y (1999) Room-temperature X- and gamma-ray detectors using thalium bromide crystals. Nucl Instrum Methods Phys Res A 436:160–164
9. Hitomi K, Shoji T, Suehiro T, Hiratate Y (1999) Radiation damage effects by 25 MeV protons and thermal annealing effects on thalium bromide nuclear radiation detectors. IEEE Trans Nucl Sci 46:213–217
10. James JE, Baciak E, He Z (2003) Comparison of 5 and 10 mm thick HgI$_2$ pixelated γ-ray spectrometers. Nucl Instrum Methods Phys Res A 505;1:191–194

11. Kaldis E (2001) Growth of mercuric iodide bulk crystals. In: Buschow KHJ (ed.) Encyclopedia of materials: Science and technology, Elsevier, Amsterdam, pp 5333–5337

12. Knoll GF (1989) Radiation detection and measurement, 2nd ed. Wiley, New York

13. Lund JC, Olschner F, Burger A (1995) Lead iodide crystals and detectors. In: Schlesinger TE, James RB (eds) Semiconductors for room temperature nuclear detector applications, semiconductors and semimetals. Vol. 43. Academic Press, San Diego, pp 443–464

14. Marcondes RM, Martins JFT, Santos RA, Costa FE, Gennari RF, Hamada MM (2011) The physical vapor transport as a technique for purification and growth of the HgI_2 crystal. In: 2011 Int Nuclear Atlantic Conf (INAC/ENAN), INAC2011, Belo Horizonte, Brazil

15. Martín-Gil J, Martín-Gil FJ, De Andrés Santos AI, Ramos-Sánchez MC, Barrio-Arredondo MT, Chebib-Abuchala N (1997) Thermal behaviour of medical grade silicone oils. J Anal Appl Pyrolysis 42;2:151–158

16. McGregor DS, Hermon H (1997) Room-temperature compound semiconductor radiation detectors. Nucl Instrum Methods Phys Res A 395;1:101–124

17. McLaughlin JP (eds) (2005) The natural radiation environment. Vol. 7. Elsevier, London

18. Oliveira IB, Costa FE, Chubaci JFD, Hamada MM (2004) Purification and preparation of TlBr crystals for room temperature radiation detector applications. IEEE Trans Nucl Sci 51:1224–1228

19. Owensa A, Bavdaz M, Brammertz G *et al*. (2003) The X-ray response of TlBr. Nucl Instrum Methods Phys Res A 497:370–380

20. Ponpon JP, Amann M (2006) Etching of mercuric iodide in cation iodide solutions. Appl Surf Sci 252;18:6313–6322

21. Rao MR, Verma JKD (1980) Solution grown mercuric iodide crystals as low-energy gamma-ray conduction type detectors. Appl Phys 13;8:1545–1550

22. Ricker GR, Vallerga JV, Wood DR (1983) A mercuric iodide detector system for X-ray astronomy: I. Design considerations and predictions of background and sensitivity. Nucl Instrum Methods Phys Res A 213:133–144

23. Ugucioni JC, Neto Ghilardi T, Mulato M (2010) Mercuric iodide crystals obtained by solvent evaporation using ethanol. Nucl Instrum Methods Phys Res A 615:259–266

24. Weiguang Y, Lei N, Dongmei L *et al*. (2011) Growth of oriented polycrystalline α-HgI_2 films by ultrasonic-wave-assisted physical vapor deposition. J Cryst Growth 324;1:149–153

25. Wilson MD, Cernik C, Chen H *et al*. (2011) Small pixel CZT detector for hard X-ray spectroscopy. Nucl Instrum Methods Phys Res A 652:158–161

26. Zhou HT, Lee CH, Chung JM, Shin CT, Chiu KC, Lan SM (2003) Growth of α-HgI_2 single crystals from physical vapor transport in an oil-bath furnace. Mater Res Bull 38;15:1987–1992